Structural Changes of Phospholipid Monolayers Caused by Coupling of Human Serum Albumin: A GIXD Study at the Air/Water Interface

ARTICLE *in* THE JOURNAL OF PHYSICAL CHEMISTRY B · AUGUST 2004

Impact Factor: 3.3 · DOI: 10.1021/jp0470243

6 AUTHORS, INCLUDING:

Qiang He
Harbin Institute of Technology
102 PUBLICATIONS **3,192** CITATIONS
SEE PROFILE

Helmuth Moehwald
Max Planck Institute of Colloids and Interfaces
1,000 PUBLICATIONS **38,295** CITATIONS
SEE PROFILE

Structural Changes of Phospholipid Monolayers Caused by Coupling of Human Serum Albumin: A GIXD Study at the Air/Water Interface

Xiaoli Wang,[†] Qiang He,[†] Suping Zheng,[†] Gerald Brezesinski,[‡] Helmuth Möhwald,[‡] and Junbai Li*[,†]

International Joint Lab, Key Lab of Colloid and Interface Science, The Center for Molecular Science, Institute of Chemistry, Chinese Academy of Sciences, Zhong Guan Cun, Beijing 100080, China and Max Planck Institute of Colloids and Interfaces, Am Mühlenberg 1, D-14476 Golm/Potsdam, Germany

Received: July 6, 2004

Phase behavior and structural changes were studied for phospholipid monolayers coupled with human serum albumin (HSA) at the air/buffer (pH 3.8) interface by film balance and grazing incidence X-ray diffraction (GIXD) measurements. For comparison, the lipid headgroup was varied from small ionic L-α-dipalmitoyl-phosphatidic acid (DPPA) to large ionic L-α-dipalmitoyl-phosphatidyl-L-serine (DPPS) and zwitterionic L-α-distearoyl-phosphatidylcholine (DSPC). The presence of HSA leads to a more or less pronounced plateau in the pressure/area isotherms of all phospholipids. GIXD diffraction patterns illustrate that the phase sequences of DPPS and DPPA on buffer (oblique−rectangular−hexagonal) are changed because of the binding of HSA. The oblique−rectangular phase transition disappears and the rectangular−hexagonal phase transition shifts to a lower surface pressure. However, there is no effect of HSA on the structure of the DSPC monolayer (NN tilted rectangular packing). Phase diagrams of DPPA/HSA, DPPS/HSA, and DSPC/HSA have been established. A tilt angle decrease in both DPPA/HSA and DPPS/HSA monolayers is observed, but no change of the tilt angle for DSPC molecules in the mixed DSPC/HSA monolayer is found. Thus, whereas HSA binding stabilizes the liquid-expanded phase at low pressures most probably via penetration, it condenses the ordered phases of anionic monolayers via reducing the headgroup repulsion. The positional correlation lengths ξ_i parallel and perpendicular to the tilt direction change because of the binding of HSA.

Introduction

Phospholipid monolayers are suitable model systems for studying a variety of questions in physical chemistry and biology. One of these is related to the lattice structure, morphology, and their changes caused by the binding and interaction with proteins or polymers.[1−5] Especially protein/phospholipid interactions at interfaces are of great interest since both proteins and phospholipids are major components of biological membranes.[6−9] Protein adsorption to interfaces plays a crucial role for many biotechnological and medical applications, for example, protein-resistant surface coatings. The forces leading to protein adsorption can be enthalpic as well as entropic. Therefore, it is important to understand the role of different forces in the adsorption process.

The most abundant plasma protein of the circulatory system, human serum albumin (HSA), contributes significantly to the osmotic blood pressure and to many transport and regulatory processes.[10−12] The three-dimensional structure of HSA has been determined crystallographically to a resolution of 2.8 Å,[13,14] which has promoted studies of binding properties of HSA. Numerous studies have focused on it with a wide variety of substrates,[15,16] ranging from metals such as calcium and copper to fatty acids, amino acids, and hormones.. Previously, we have studied the dynamic adsorption process of HSA into an assembled lipid monolayer.[17,18]

Theoretical simulation of the human serum albumin (HSA) to gain insight into its association with either neutral or negatively charged lipids or liposomes has been performed by other groups serving as a model to better understand the interaction of lipids and proteins.[19]

In the present work, we combined the technique of grazing incidence X-ray diffraction (GIXD) with film balance measurements to demonstrate that binding of HSA to charged lipids results in changes of both phase sequence and structure of lipid monolayers, whereas HSA binding to zwitterionic lipids does not change the monolayer structure.

The motivation for this work is basically a physicochemical one, however, one may also conclude on physiological conditions, although the work has been performed at pH 3.8. Under our conditions, membrane and HSA are oppositely charged; hence, electrostatic attraction is most pronounced. At pH 7 we expect only weak interactions; thus, the effects measured here may be considered as upper limits. On the other hand, there might be significant differences between the pH at the interface with respect to the subphase pH. Therefore, this study should give an answer on the question about the role of electrostatic interactions on HSA binding to lipid surfaces.

Experimental Section

Materials. L-α-Dipalmitoyl-phosphatitic acid (DPPA, +99%), L-α-dipalmitoyl-phosphatidyl- L-serine (DPPS, approximately 98%), L-α-distearoyl-phosphatidylcholine (DSPC, +99%), and human serum albumin (HSA, essentially fatty acid free, ≥96% albumin, catalog number: A1887) were purchased from Sigma

* Corresponding author. Tel: +86 10 82614087; fax: +86 10 82612484; e-mail: jbli@iccas.ac.cn.
[†] Chinese Academy of Sciences.
[‡] Max Planck Institute of Colloids and Interfaces.

10.1021/jp0470243 CCC: $27.50
Published on Web 08/24/2004

SCHEME 1: Chemical Structures of 1,2-Dipalmitoyl-phosphatitic Acid (DPPA) (a), Dipalmitoyl-phosphatidyl-L-serine (DPPS) (b), and 1,2-Distearoyl-phosphatidylcholine (DSPC) (c) and Schematic Representation of Human Serum Albumin (HSA) (d)[a]

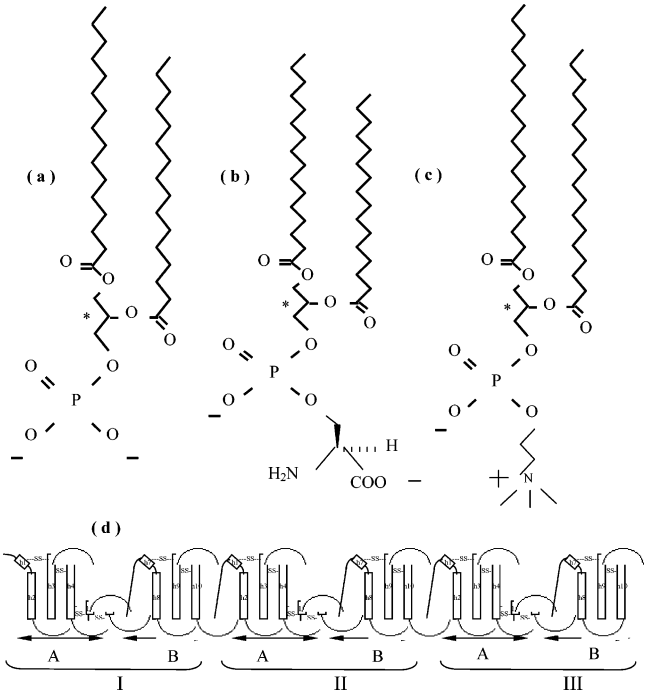

[a] This can be divided into three major domains (I, II, and III) each of which can be further subdivided into subdomains (A, B). The 10 principal helices in each domain are labeled as h1−h10.[7]

and used without further purification. DPPA and DPPS were dissolved in chloroform/methanol v:v = 7:3 (for HPLC with 99.9% purity, purchased from Promochem GmbH, Germany), and DSPC was dissolved in pure chloroform.

The chemical structures of DPPA, DPPS, and DSPC and a schematic representation of human serum albumin (HSA) are shown in Scheme 1. Domains I−III of the HSA molecule are structurally homologous.[13] Each is composed of two subdomains referred to as A and B, formed by three to four α-helices linked by a long section of an α-helix.[14] Subdomains IA, IB, and IIA pack tightly, forming an enlarged head for the molecule, whereas subdomains IIB, IIIA, and IIIB form the extended tail. The binding cavities in IIIA and IIA are more active, especially the binding cavity in IIIA which is the most active and accommodating in HSA.[13,14] Many ligands were found to bind preferentially there. This kind of binding to domain IIIA and IIA often affects conformational changes because the binding subdomains share a common interface. Generally, HSA has a greater affinity for small, negatively charged hydrophobic molecules.[13,15] For example, HSA is the principal carrier of fatty acids in the blood. According to the pH dependent study of HSA molecular subdomains,[20] the HSA molecule should exhibit a rather extended configuration with a large accessible area in buffer at pH 3.8 (between 2.7 and 4.3), and should be in the form of F (fast) with the α-helical content being 45%, partially unfolding and expanding because of mutual repulsion of the subdomains.[21]

The water used in all experiments was Millipore-filtered. Buffer solutions prepared with H_3PO_4 and NaOH were adjusted to pH 3.8 using 1 M HCl. The protein concentration was 1×10^{-8} M. All experiments were performed at (20.0 ± 0.1) °C controlled by a thermostat.

Isotherm Measurements. The pressure−area isotherms of the coupled DPPA/HSA, DPPS/HSA, and DSPC/HSA monolayers were determined 3 h after protein adsorption in an LB trough (R&K, Wiesbaden, Germany) equipped with a Wilhelmy pressure measuring system. The compression rate was 0.05 Å^2/(molecule·s).

GIXD Measurements. The grazing incidence X-ray diffraction experiments were carried out using the liquid-surface diffractometer on the undulator beamline BW1 at HASYLAB, DESY (Hamburg, Germany).[22] The experimental setup was the same as described elsewhere.[22] The monolayer can be considered as a two-dimensional powder. The beam was made monochromatic by a beryllium crystal (002) and adjusted to strike the surface with an angle of incidence $\alpha_i = 0.11°$. The diffracted intensity was detected by a linear position-sensitive detector (PSD) (OED-100-M, Braun, Garching, Germany) as a function of the vertical scattering angle α_f.[24] To record the intensity as a function of the horizontal scattering angle 2θ, this detector was rotated around the sample. The in-plane divergence of the diffracted beam was restricted to 0.09° by a Soller collimator in front of the PSD. The scattering vector **Q** is given in terms of an in-plane (or horizontal) component $\mathbf{Q}_{xy} = (2\pi/\lambda)\sqrt{\cos^2\alpha_i+\cos^2\alpha_f-2\cos\alpha_i\cos\alpha_f\cos 2\theta}$ and an out-of-plane (or vertical) component $\mathbf{Q}_z = (2\pi/\lambda)(\sin\alpha_i + \sin\alpha_f)$, where λ is the X-ray wavelength.[22−26] The intensities as a function of $\mathbf{Q}_{xy}$ and $\mathbf{Q}_z$ were least-squares fitted as a Lorentzian in the in-plane direction and as a Gaussian in the out-of-plane direction.

From the peak positions, the lattice parameters *a*, *b*, and γ, the unit cell area A_{xy}, the cross-sectional area of alkyl chains A_0, and the tilt angle *t* can be calculated.[23] The positional correlation lengths ξ_i are obtained from the full width at half-maximum (fwhm) of the in-plane component of the scattering vector.[27]

The measurements were performed 3 h after protein adsorption to work at the same conditions as for the pressure/area isotherms. The starting surface pressure of the coupled phospholipid/HSA monolayers was always around zero mN/m.

Results and Discussion

The $\pi-A$ isotherms of DPPA, DPPS, and DSPC monolayers on HSA solution can be compared with those of the lipid monolayers on buffer as shown in Figure 1. At 20 °C and high pressures, all lipids investigated exhibit fully condensed isotherms on the buffer used. Obviously, the coupling of HSA to DPPA or DPPS shifts the isotherms to much larger molecular areas at low surface pressures, and additionally a plateau region appears in the isotherms. This directly reflects the effect of penetration and binding of HSA molecules to the charged DPPA and DPPS monolayers. The coupling of DSPC to HSA molecules also shifts the isotherm to larger areas per molecule, and a kind of plateau appears around 20 mN/m.

Figure 2A and 2B shows the diffraction pattern of DPPA on buffer and on HSA, respectively. A phase sequence oblique−rectangular−hexagonal was observed on buffer, whereas the DPPA/HSA monolayer exhibits at very low surface pressure already a centered rectangular structure, which changes into a hexagonal one on compression.

Figure 3 shows the contour plots of DPPS on buffer (A) and on HSA solution (B) at different surface pressures. On buffer, three diffraction peaks are observed at lower pressures indicating that the chains of DPPS molecules are tilted in an intermediate direction between NN (nearest neighbors) and NNN (next-nearest neighbors) below at least 13 mN/m, where a kink was

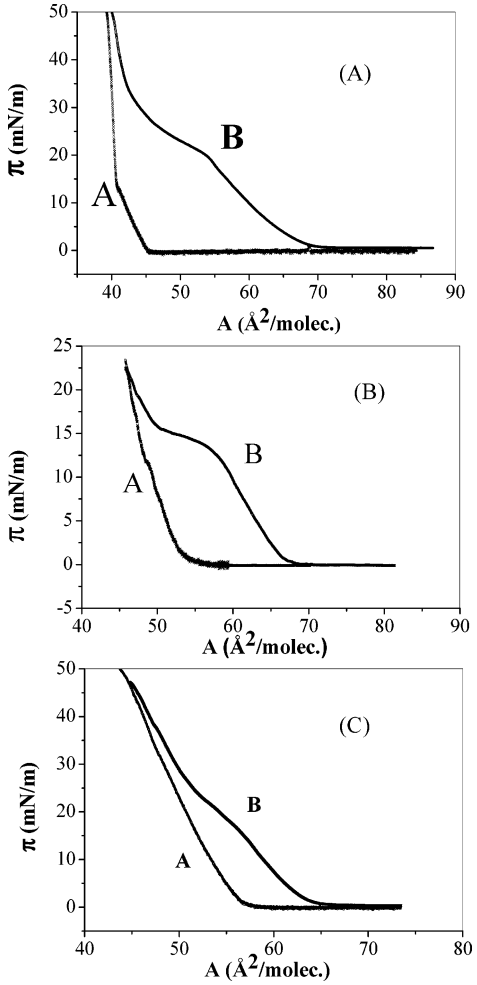

Figure 1. $\pi-A$ isotherms of DPPA (A), DPPS (B), and DSPC (C) on buffer and on HSA solution, respectively.

found in the isotherm (Figure 3A). As the surface pressure was increased to 16 mN/m, two diffraction peaks are observed indicating that the hydrophobic chains of DPPS molecules are now packed in a rectangular unit cell with NN tilt direction. At high pressure, the DPPS chains are untilted and hexagonally packed. The corresponding $\mathbf{Q}_{xy}$ and $\mathbf{Q}_z$ data are given in Table 1. The results reveal that the lattice of the pure DPPS monolayer on buffer is changing from oblique to rectangular and finally to hexagonal on compression.

Figure 3B shows the X-ray data of the coupled DPPS/HSA monolayer at $\pi \geq 15$ mN/m where the new plateau in the isotherm appeared (see Figure 1). No structure corresponding to a regular chain arrangement in the coupled DPPS/HSA monolayer was observed below this surface pressure (Figure 3B(I)). Above 15 mN/m, a rectangular packing with NN tilt direction was observed in the LC phase of the DPPS/HSA monolayer (Figure 3B(II) and 3B(III)). The hexagonal packing of untilted molecules can be seen at 30 mN/m in the mixed DPPS/HSA monolayer (Figure 3B(IV)). Obviously, coupling of HSA destroys the condensed monolayer structure leading to a liquid-expanded phase, which is not observed for the DPPS monolayer on buffer.

For the mixed DSPC/HSA monolayer, the X-ray measurements show that two distinct scattering peaks appear at all pressures investigated. As shown in Figure 4A and 4B, the diffraction patterns of the pure DSPC and mixed DSPC/HSA monolayers are very similar. The observed structure is rectangular with the chains of DSPC molecules tilted in NN direction.

TABLE 1: Maximum Positions of Bragg Peaks and Rods (Q_{xy}, Q_z) and fwhm (Below Each Peak Position) for DPPS, DPPA, DSPC on Buffer and on HSA Solution at Different Surface Pressures

π, mN/m	$Q_{xy}1$, Å^{-1}	ΔQ_{xy}	Q_z1, Å^{-1}	ΔQ_z	$Q_{xy}2$, Å^{-1}	ΔQ_{xy}	Q_z2, Å^{-1}	ΔQ_z	$Q_{xy}3$, Å^{-1}	ΔQ_{xy}	Q_z3, Å^{-1}	ΔQ_z
					DPPS/buffer							
2	1.478		0.067		1.447		0.493		1.407		0.560	
	0.014		0.28		0.029		0.28		0.030		0.28	
5	1.484		0.056		1.456		0.457		1.422		0.513	
	0.019		0.28		0.024		0.28		0.027		0.28	
9	1.489		0.043		1.467		0.421		1.439		0.464	
	0.018		0.28		0.019		0.28		0.026		0.28	
13	1.495		0.037		1.478		0.364		1.459		0.401	
	0.012		0.28		0.021		0.28		0.028		0.28	
16	1.499		0		1.477		0.341					
	0.019		0.28		0.042		0.28					
20	1.505		0		1.496		0.241					
	0.013		0.28		0.034		0.28					
30	1.515		0									
	0.016		0.28									
					DPPS/HSA							
20	1.500		0		1.486		0.291					
	0.015		0.29		0.043		0.29					
25	1.505		0		1.496		0.211					
	0.013		0.29		0.029		0.29					
30	1.515		0									
	0.018		0.29									
40	1.517		0									
	0.018		0.29									
					DPPA/buffer							
10	1.501		0.014		1.494		0.303		1.470		0.317	
	0.012		0.29		0.028		0.29		0.028		0.29	
15	1.506		0		1.499		0.162					
	0.017		0.28		0.047		0.28					
25	1.516		0									
	0.018		0.27									
					DPPA/HSA							
0.4	1.512		0		1.481		0.075					
	0.011		0.29		0.04		0.29					
6	1.515		0									
	0.014		0.29									
20	1.520		0									
	0.014		0.27									
					DSPC/buffer							
15	1.451		0		1.304		0.840					
	0.011		0.27		0.057		0.27					
25	1.456		0		1.333		0.795					
	0.012		0.27		0.051		0.27					
35	1.461		0		1.363		0.740					
	0.012		0.26		0.047		0.26					
45	1.466		0		1.389		0.667					
	0.013		0.26		0.049		0.26					
					DSPC/HSA							
15	1.452		0		1.309		0.835					
	0.011		0.27		0.054		0.27					
22.6	1.456		0		1.334		0.792					
	0.011		0.27		0.048		0.27					
35	1.467		0		1.364		0.724					
	0.013		0.26		0.044		0.26					
45	1.467		0		1.390		0.663					
	0.013		0.26		0.045		0.26					

Table 1 gives the peak positions of the in-plane and out-of-plane components of the scattering vector ($\mathbf{Q}_{xy}$, $\mathbf{Q}_z$) and the corresponding full width at half-maximum (fwhm) for DPPA, DPPS, and DSPC both on buffer and on HSA.

The tilt angles as a function of surface pressure are plotted in Figure 5 for DPPA, DPPS, and DSPC on buffer and on the HSA solution. These phase diagrams show that in the negatively charged lipid monolayers the coupling with HSA leads to drastic changes in the tilt angle. In contrast, HSA does not have any

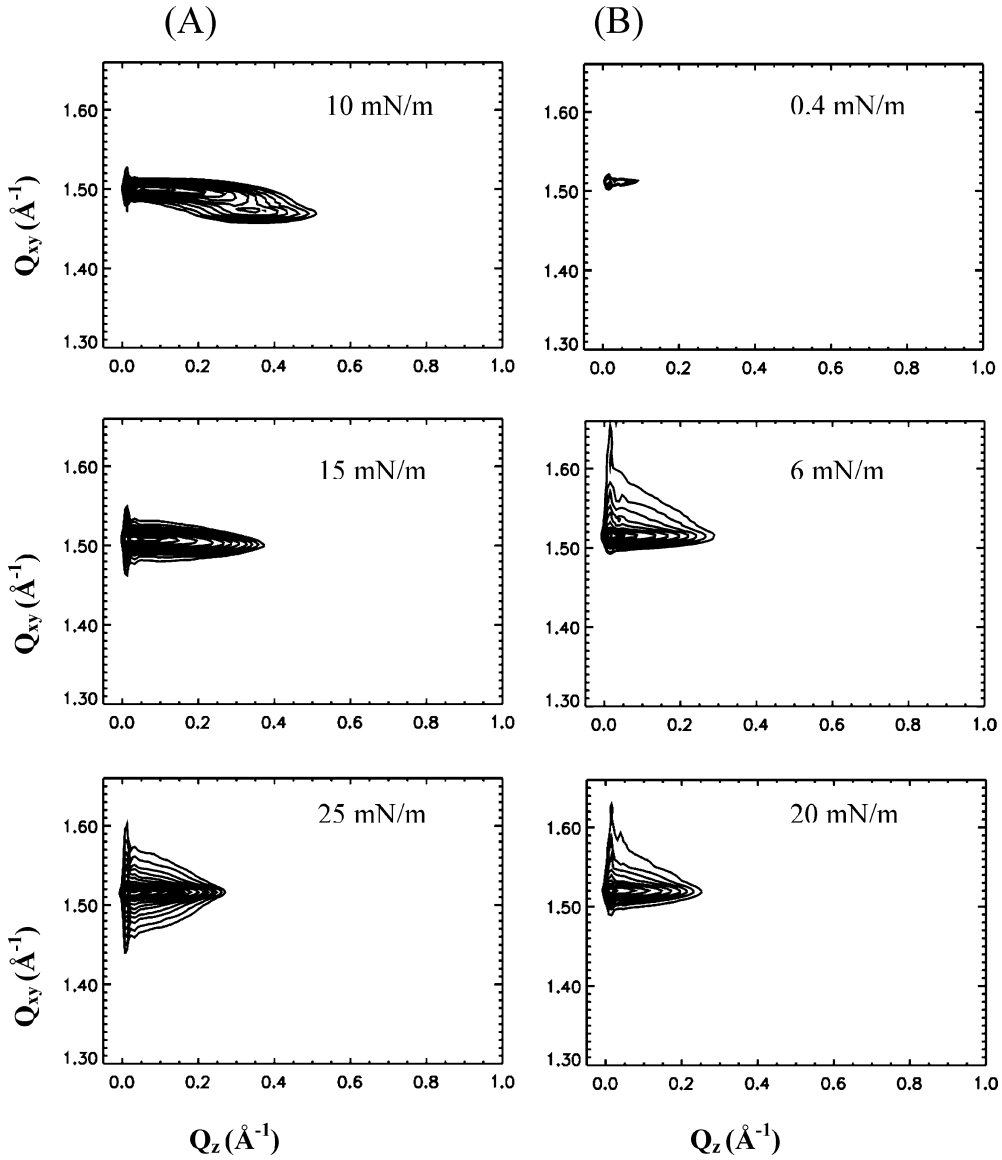

Figure 2. Contour plots of the corrected X-ray intensities vs in-plane and out-of-plane scattering vector components $\mathbf{Q}_{xy}$ and $\mathbf{Q}_z$ for DPPA on buffer (A) and on HSA solution (B) at different surface pressures (indicated).

effect on the packing of the zwitterionic DSPC. Mainly, the electrostatic interactions between the anionic lipids and the oppositely charged HSA seem to be responsible for the structural changes.

For DPPA (Figure 5A) at low pressure, the tilt angles on the two subphases are almost the same. At higher pressures, there are distinct differences. The phase sequence oblique−rectangular−hexagonal can be observed on water as well as on buffer, however, the two phase transitions are shifted to lower surface pressures. Coupling with HSA leads to a drastic decrease of the tilt angle. Only at the lowest pressure close to zero a small tilt of about 3 degrees can be observed. The phase transition from a centered rectangular lattice to hexagonal packing of untilted chains occurs already between 1 and 5 mN/m.

The observed phase sequence of DPPS on buffer is the same as for DPPA on buffer, that is, oblique−rectangular−hexagonal (Figure 5B). When binding with HSA, the oblique phase disappears and the transition between the tilted rectangular (L_2) and the untilted hexagonal structure (LS) is shifted to lower surface pressure. Comparing the same surface pressure, the tilt angle on the HSA solution is about 5° smaller compared with that on buffer or the corresponding pressure is reduced about 3 mN/m. The disappearance of the oblique phase indicates that the DPPS/HSA electrostatic interactions can have a strong effect on, for example, chiral interactions between the phospholipid headgroups, which are in many cases responsible for oblique structures, by changing the conformation of the DPPS headgroup. On the other hand, electrostatic screening also plays an important role. Sodium and hydrogen ions in the buffer and HSA molecules with charges opposite to those of the phospholipid headgroups can screen the electrostatic repulsion between anionic headgroups leading to more compact packing in the monolayer. Changed headgroup conformations allow decreasing of the tilt angle of the chains. In contrast to DPPA, interactions between DPPS and HSA lead even to a fluidization of the monolayer at low surface pressure. No structure can be observed below 15 mN/m. Therefore, the plateau in the isotherm at 15 mN/m indicates a first-order transition between liquid-expanded and condensed phases. In DPPA and DSPC, the plateau in the isotherms, which appears around 20 mN/m, is an indication of a squeezing-out of HSA from the monolayer. This plateau is much more pronounced for DPPA compared with DSPC, because there are much stronger interactions between HSA and the anionic phospholipids.

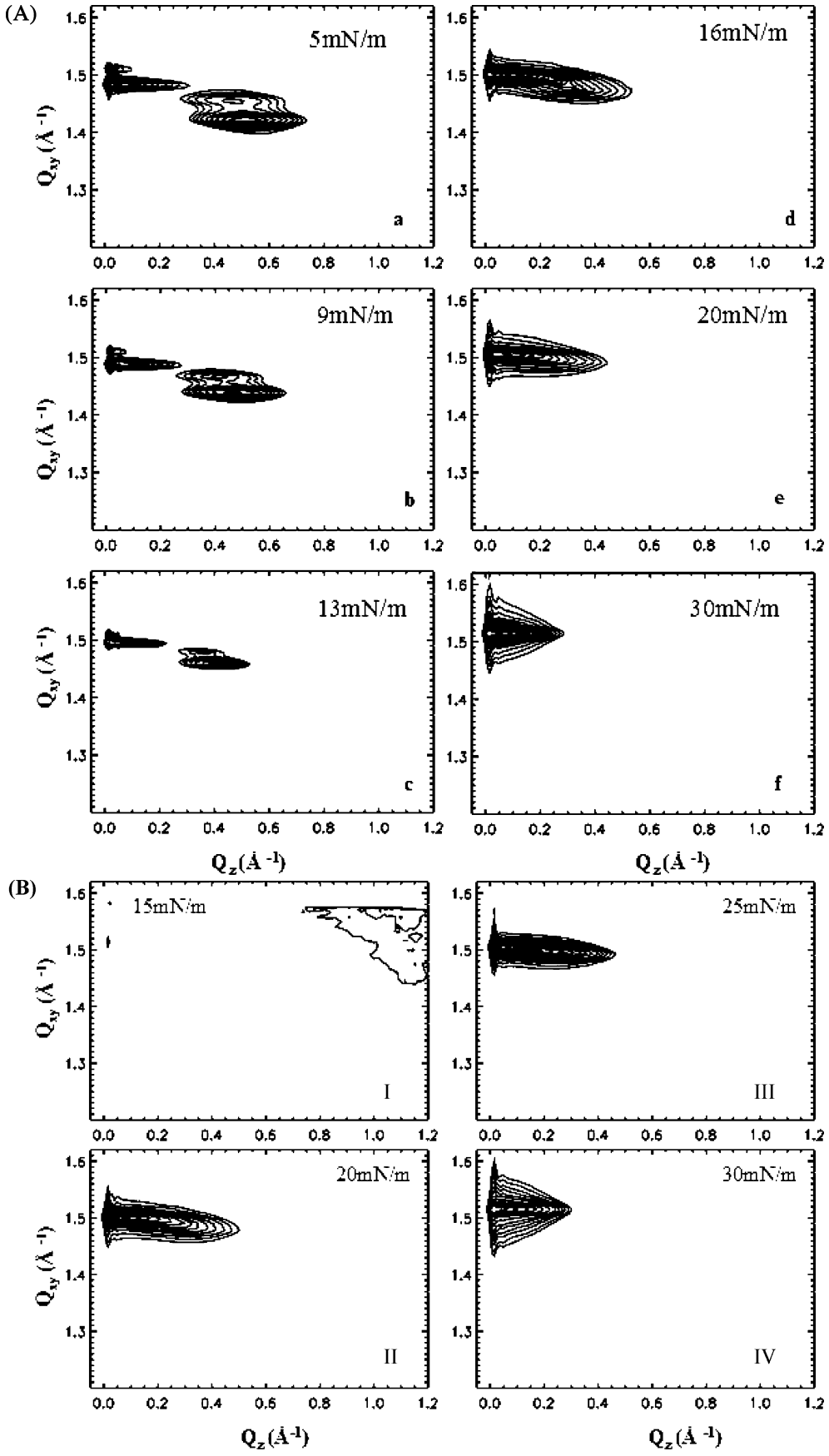

Figure 3. Contour plots of the corrected X-ray intensities vs in-plane and out-of-plane scattering vector components $\mathbf{Q}_{xy}$ and $\mathbf{Q}_z$ for DPPS on buffer (A) and on HSA solution (B) at different surface pressures (indicated).

At pH 3.8, the HSA molecule should exhibit a rather extended configuration with a large accessible area and there are more free positive charges in domains I, II, and III (i.e., $p \approx 4.8$),[20] especially the free charges of domain III should be much more than +2e.[27] HSA may undergo an internal conformational change to facilitate binding with lipid monolayers. Figure 5B

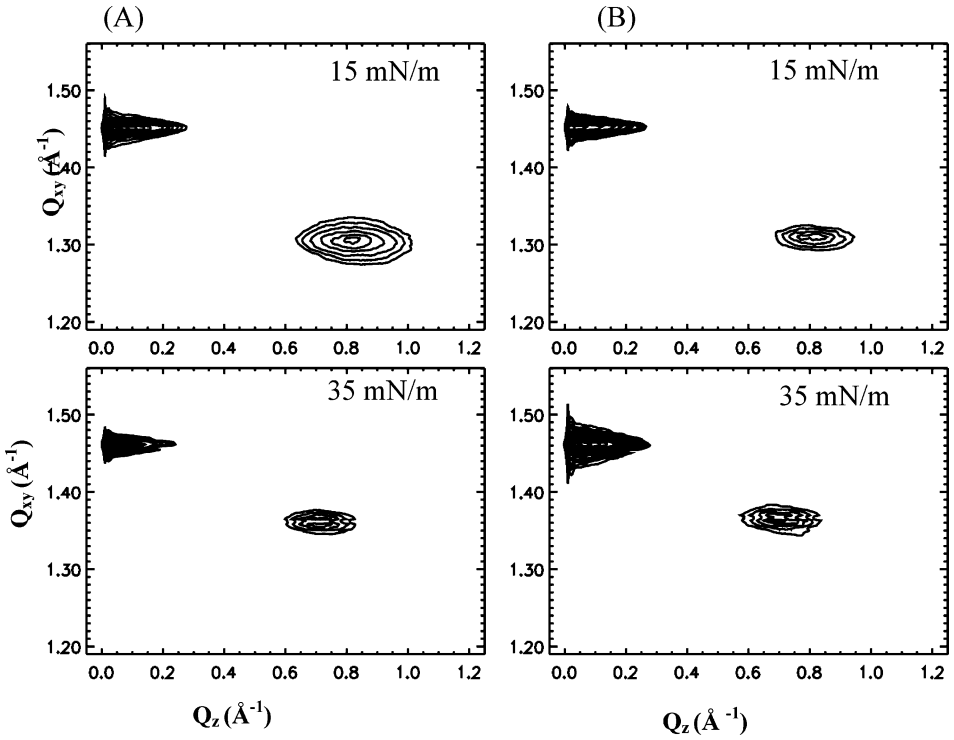

Figure 4. Contour plots of the corrected X-ray intensities vs in-plane and out-of-plane scattering vector components $\mathbf{Q}_{xy}$ and $\mathbf{Q}_z$ for DSPC on buffer (A) and on HSA solution (B) at different surface pressures (indicated).

shows that HSA binding effectively causes a pressure change of $\Delta\pi \sim 3$ mN/m. This corresponds to a change in surface energy ΔE per molecule with an area of $A = 45$ Å^2; $\Delta E = \Delta\pi^* A = 3$ (mN/m)* 45*10^{-20} (m^2) ≈ 10 meV. This value is not untypical for electrostatic interactions in water. Although it is below k_BT, it may be very important considering that the proteins interact over a larger area with cooperative units of roughly 100 molecules. Then, the resulting energy of about 1 eV, being well above $k_BT = 25$ meV, may cause considerable structural changes.

Figure 5C shows the phase diagram of DSPC on buffer and on HSA solution. Both systems exhibit the same diffraction patterns (see Figure 4). The tilt angle decreases in the same way with increasing surface pressure: from 37.8° to 29.5° as the surface pressure increases from $\pi = 15$ to 45 mN/m. No phase transition is found and the structure remains centered rectangular with NN tilt (L_2 phase). The GIXD results demonstrate that the interaction of DSPC with HSA must be rather weak. There are no electrostatic interactions between the large and strongly hydrated zwitterionic headgroups of DSPC and HSA molecules. The shift to larger molecular areas seen in the isotherm can be only ascribed to the penetration of HSA without any specific interaction.

The positional correlation lengths ξ in the same phase, calculated from the fwhm of the Bragg peaks, also yield interesting results on the direction of the coupling. In agreement with a general phenomenon with Langmuir monolayers, the positional correlation lengths ξ in DPPA, DPPS, or DSPC monolayer are much shorter in tilt direction than perpendicular to it, which has been ascribed to a one-dimensional crystallization and to weak interaction along the tilt direction.[4,16,2] In the L_2 phase (rectangular unit cell and NN tilt), both in the presence and absence of HSA, the correlation length increases with increasing pressure. Binding of HSA leads to a drastic change in the ratio between the correlation lengths perpendicular and parallel to the tilt direction. For example, for DPPA, this ratio decreases from 2.7 in the absence of HSA to 1.5 in the presence of HSA. This suggests that coupling of HSA molecules leads to a more uniform ordering in the phospholipid monolayer. For DPPS, this ratio increases from 0.9 in the absence of HSA to 2.2 in the presence of HSA. This indicates that the binding of HSA molecules with DPPS monolayers occurs preferentially in a direction nearly perpendicular to the chain tilt, which leads to a higher order perpendicular to the tilt direction but creates more defects parallel to the direction of the molecular tilt. This is an additional indication for a different interaction of HSA with DPPS compared with DPPA. In DSPC, one observes that there is only a small influence of HSA on the correlation lengths. By comparing the influence of HSA on the ordered phases of DPPA and DPPS, one realizes that the influence on the latter system is less pronounced. This is probably because that even if the electrostatic repulsion is screened the bulkier phosphatidylserine group still resists compression, and this is also reflected in the isotherm. The latter has a less steep slope and even at the highest pressure does not reach the limiting area of 40 Å^2. Hence, whereas HSA coupling to DPPS effectively reduces the repulsive pressure of the headgroups by about 3 mN/m, the coupling to DPPA reduces it by about 15 mN/m. This again demonstrates that the specific nature of the headgroup is most important.

In summary, the present work provides direct evidence for the interaction of different phospholipids (DPPA, DPPS, and DSPC) with HSA in monolayers at the air/water interface. The GIXD data obtained show that HSA changes the diffraction patterns and phase sequences of phospholipid monolayers differently. A pronounced change in the tilt angle of DPPA and DPPS was found while no change was observed in DSPC. On the basis of the correlation lengths derived from the X-ray measurements, it is deduced that HSA binding to DPPA leads to a more uniform lattice, whereas HSA binding to DPPS monolayer increases the order preferentially in a direction nearly perpendicular to the tilt. Obviously, the interactions of the anionic phospholipids with HSA are mainly caused by electrostatic forces. The experiments demonstrate that HSA does not

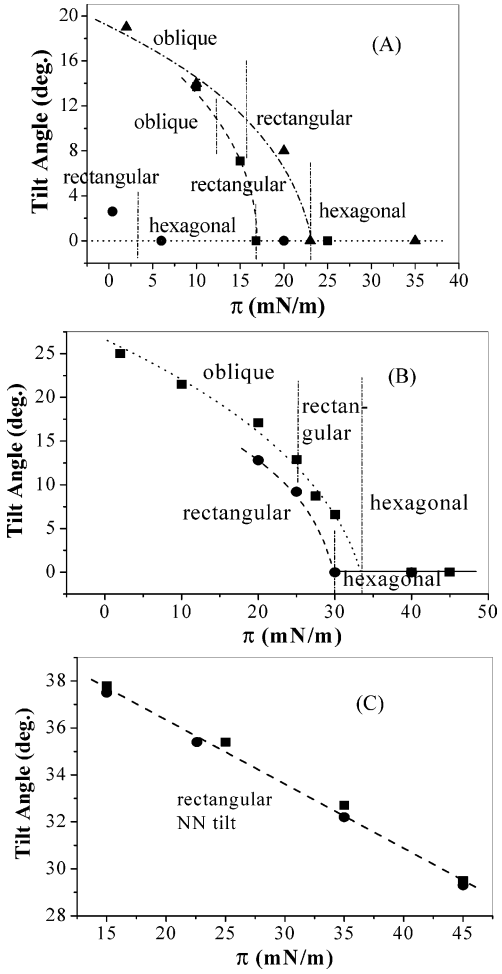

Figure 5. Phase diagrams (tilt angle *t* as a function of lateral pressure π) of DPPA (A), DPPS (B) and DSPC (C) monolayers on pure water (▲), buffer (■) and HSA solution (●), respectively.

simply insert into the anionic monolayer (increase of molecular area) but attaches to the headgroups and changes their arrangement, which leads to smaller tilt angles of the chains. Comparing DPPA/buffer with DPPA/HSA, one observes that the decrease of the tilt angle with increasing surface pressure is much more pronounced because of the binding with HSA molecules than because of screening of headgroup repulsion merely by buffer ions. This indicates that the influence of HSA molecules is reduced headgroup repulsion, stronger than that due to salt ions.

The absence of lattice changes of the zwitterionic DSPC on the HSA subphase indicates that there are no interactions or that possible interactions with both the hydrophobic and hydrophilic regions of the phospholipid monolayer compensate. Since the experiments have been made at unphysiological pH, we should comment on the biological significance of the results. At pH 7 HSA, DPPA and DPPS are negatively charged, hence, one expects weaker binding to the interface. If this exists at all, for example, by dipolar or hydrophobic interactions, the influence measured in this work may be considered as an upper limit. This work therefore represents a thorough physicochemical study showing that under physiological conditions HSA has only a weak influence on the membrane structure. It may penetrate a membrane with loosely packed aliphatic tails but will not distort the ordered phases.

Acknowledgment. This work was financially supported by the National Nature Science Foundation of China (NNSFC29925307 and NNSFC90206035) as well as the collaboration project of the German Max Planck Society. We thank HASYLAB (DESY, Hamburg, Germany) for providing beamtime and Kristian Kjaer (Risoe) for help at the beamline BW1.

References and Notes

(1) Sheller, N. B.; Petrash, S.; Foster, M. D. *Langmuir* **1998**, *14*, 4535.
(2) *Protein−Lipid Interactions, New Comprehensive Biochemistry* (Review); Watts, A., Ed.; Elsevier: Amsterdam (Review), 1993; Vol. 25.
(3) Martin, B.; Nylander, T.; Arnebrant, T.; Clark, D. C. Protein/Emulsifier Interactions. *Food Emulsifiers and Their Applications* (Review); 1996; Chapter 5, pp 95−146.
(4) Meijere, K. de; Brezesinski, G.; Moehwald, H. *Macromolecules* **1997**, *30*, 2337.
(5) Meijere, K. de; Brezesinski, G.; Kjaer, K.; Moehwald, H. *Langmuir* **1998**, *14*, 4204.
(6) Cornell, D. G. J. *Colloid Interface Sci.* **1982**, *88*, 536.
(7) Bos, M. A.; Kleijn, J. M. *Biophys. J.* **1995**, *68*, 2566.
(8) Kleijn, J. M. *Biophys. J.* **1995**, *68*, 2572.
(9) Lu, B.; Wei, Y. J. *Colloid Interface Sci.* **1993**, *161*, 120.
(10) Grase, T. G.; Pierce, J. A.; Cooper, S. L. J. *Biomed. Mater. Res.* **1987**, *21*, 815.
(11) Munro, M. S.; Eberhart, R. C.; Maki, N. J.; Brink, B. E.; Fry, W. J. *J. Am. Soc. Artif. Intern. Organs* **1983**, *6*, 65.
(12) Lyman, D. J.; Knutson, K.; McNeil, B.; Shibatani, K. *Trans. Am. Soc. Artif. Intern. Organs* **1975**, *21*, 49.
(13) He, X. M.; Carter, D. C. *Nature* **1992**, *358*, 209.
(14) Carter, D. C.; He, X. M.; Munson, S. H.; Twigg, P. D.; Gernert, K. M.; Broom, M. B.; Miller, T. Y. *Science* **1989**, *244*, 1195.
(15) Carter, D. C.; Ho, J. X. *Advances in Protein Chemistry*; Academic Press: New York, 1994; vol. 45, p 153.
(16) Spector, A. A. *J. Lipid Res.* **1975**, *16*, 165.
(17) Wang, X. L.; Zhang, H. J.; Cui, G. C.; Li, J. B. *J. Mol. Liq.* **2001**, *90*, 149.
(18) Wang, X.; Zhang, Y.; Wang, M. Q.; Cui, G. C.; Li, J. B.; Brezesinski, G. *Colloids Surf., B* **2001**, *23*, 91−94.
(19) Olivieri, J. R.; Craievich, A. F. *Eur. Biophys. J.* **1995**, *24*, 77.
(20) Foster, J. F. In *Albumin Structure, Function, and Uses*; Rosenoer, V. M., Oratz, M., Rothschild, M. A., Eds.; Pergamon: Oxford, 1977; pp 53−84.
(21) Kjaer, K. *Experimental Stations at HASYLAB*; January 1994; pp 88−89
(22) De Wolf, C.; Bringezu, F.; Brezesinski, G.; Möhwald, H.; Howes, P.; Kjaer, K. *Physica B* **1998**, *248*, 199.
(23) Als-Nielsen, J.; Möhwald, H. In *Handbook on Synchrotron Radiation*; Ebashi, S., Koch, M., Rubenstein, E., Eds.; Elsevier: Amsterdam, Oxford, New York, Tokyo, 1994; Vol. 4, pp 1−53.
(24) Kjaer, K. *Physica B* **1994**, *198*, 100.
(25) Als-Nielsen, J.; Jacquemain, D.; Kjaer, K.; Lahav, M.; Leiveiller, F.; Leiserowitz, L. *Phys. Rep.* **1994**, *246*, 251.
(26) Helm, C. A.; Möhwald, H.; Kjaer, K.; Als-Nielsen, J. *Biophys. J.* **1987**, *381*, 52.
(27) Peters, T. *J. Adv. Protein Chem.* **1985**, *37*, 161.
(28) Brezesinski, G.; Struth, B.; Bringezu, F.; Scalas, E.; Möhwald, H.; Gehlert U.; Weidemann, G.; Vollhardt, D. *J. Phys. Chem.* **1995**, *99*, 8758.